Sources and holes in a one-dimensional traveling-wave convection experiment

Pastur, L.; Westra, M.T.; Water, W. van de; Hecke, M.L. van; Storm, C.; Saarloos, W. van

Sources and holes in a one-dimensional traveling-wave convection experiment

Luc Pastur,[1] Mark-Tiele Westra,[1] Daniel Snouck,[1] Willem van de Water,[1] Martin van Hecke,[2] Cornelis Storm,[3] and Wim van Saarloos[3]

[1]*Physics Department, Eindhoven University of Technology, Postbus 513, 5600 MB Eindhoven, The Netherlands*

[2]*Kamerlingh Onnes Laboratory, Universiteit Leiden, Postbus 9504, 2300 RA Leiden, The Netherlands*

[3]*Instituut-Lorentz, Universiteit Leiden, Postbus 9506, 2300 RA Leiden, The Netherlands*

(Received 8 November 2001; revised manuscript received 19 December 2002; published 25 March 2003)

We study dynamical behavior of local structures, such as sources and holes, in traveling-wave patterns in a very long (2 m) heated wire convection experiment. The *sources* undergo a transition from stable coherent behavior to erratic behavior when the driving parameter ε is *decreased*. This transition, as well as the scaling of the average source width in the erratic regime are both qualitatively and quantitatively in accord with earlier theoretical predictions. We also present results for the *holes* sent out by the erratic sources.

DOI: 10.1103/PhysRevE.67.036305 PACS number(s): 47.20.Bp, 07.05.Kf, 47.20.Dr, 47.54.+r

Traveling-wave systems play an exceptional role within the field of pattern formation. If the transition to patterns is supercritical (forward), the dynamics close to threshold should be amenable to a description by the complex Ginzburg-Landau (CGL) amplitude equation [1]. Theory and experiments are difficult to compare, however, for the following two reasons.

(i) Both the CGL model and experimentally observed traveling-wave patterns exhibit an astonishing variety of ordered, disordered, and chaotic dynamics, which can be difficult to characterize or compare.

(ii) The dynamics depends, in general, strongly on nonuniversal coefficients [2–4], but the values of these coefficients are difficult to determine in experiments [5–7].

The study of *local structures*, such as sources, fronts, and holes, which play an important role in traveling-wave systems [1–4,7–12], provide a promising route to compare theory and experiment as they partially circumvent these difficulties: their nontrivial behavior often depends only on a *subset* of the coefficients [11] and is, in addition, relatively easy to characterize experimentally [7–9,12].

In this paper, we present a successful example of this approach in a heated wire convection experiment (Fig. 1). This system forms left and right traveling waves that suppress each other; typical states consist of patches of left and right traveling waves separated by sources (which send out waves) and sinks (which have two incoming waves) [13]. An earlier theoretical work [14], which was based on the amplitude equations (1) and (2) below, predicts that, essentially due to the transition from an absolute to a convective instability [15], sources tend to display a diverging width when the driving parameter ε is lowered beyond a critical value [Eq. (3)]. More recently, it was predicted that just before these stationary sources would diverge, they become unstable and give way to *fluctuating sources* of finite average width which display highly nontrivial dynamics [4].

We indeed observe this nontrivial change in source behavior when the driving (heating of wire) is decreased; not only the measured transition value, but also the qualitative behavior of sources is in accord with the predictions [14,4]. All properties necessary to compare theory and experiment are measured in a set of independent experiments. The fluctuating sources send out *holes*, and we show that these display behavior very similar to that predicted for homoclinic holes [3].

I. EXPERIMENTAL SETUP

Our experiment consists of a 2 m long heated wire of diameter of 0.2 mm and resistivity of 50 $\Omega\,\mathrm{m}^{-1}$ that is placed under the free surface of the fluid at a depth $h=2$ mm (see Fig. 1). The wire is stretched to the breaking limit and its maximum sagging is 0.1 mm. The heat Q dissipated in the wire drives the system, through a combination of gravity- and surface-tension-induced convection, surface waves emerge at $Q=Q_c$ that travel along the wire [12]. The sides of our cell are made of brass and contain copper tubes through which cooling water of $21.0\pm0.1\,^{\circ}\mathrm{C}$ is circulated. In order to guarantee a clean, uncontaminated free surface, we use a low-viscosity, low-surface-tension silicon oil [16].

A sensitive linear measurement of the surface slope along the cell is obtained by recording the reflection of a laser beam off the fluid surface onto a position sensitive device. Both laser and position detector are mounted on a computer-controlled cart that travels on precision stainless steel rods. This allows us to measure surface wave amplitudes as small as 0.5 μm. The signals of the scanning device are wave frequency and Hilbert transformed to yield the complex valued field $A(x,t)=|A|\exp(i\phi)$. From this, the local wave number is computed as $q(x,t)=\partial\phi(x,t)/\partial x$. To improve the signal to noise ratio, running averages over a time interval of 10 s are performed.

Vince and Dubois [12] already demonstrated that the primary bifurcation at $Q=Q_c$ is supercritical and explored the phase diagram as a function of Q and wire depth h. For $\varepsilon \lesssim 0.15$, the amplitude exhibits the scaling $|A|\sim\varepsilon^{1/2}$. This is expected near a supercritical bifurcation, and it also sets the range of applicability of the amplitude description.

II. AMPLITUDE EQUATIONS

For systems with counterpropagating waves, the appropriate amplitude equations are the coupled one-dimensional CGL equations [1]:

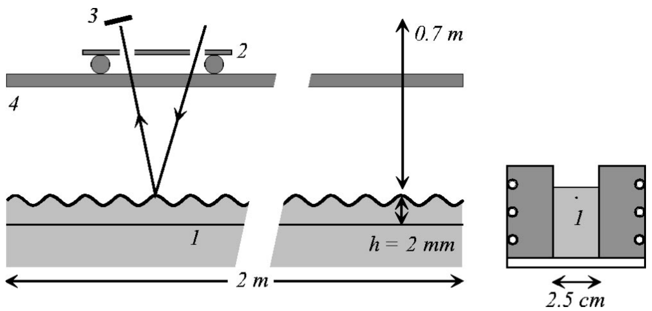

FIG. 1. Schematic side view and cross section of the heated wire experiment. A thin (0.2 mm diameter) wire, 1, is stretched beneath the free surface of a fluid (depth $h=2$ mm). When it is heated by sending an electrical current through it, surface waves are excited. The slope of the waves is measured by reflecting a laser beam off the surface onto a position sensitive detector (PSD), 3. The laser and the PSD are mounted on a cart, 2, that rides on precision steel rods, 4.

$$\tau_0(\partial_t A_R + s_0 \partial_x A_R) = \varepsilon A_R + \xi_0^2(1+ic_1)\partial_x^2 A_R - g_0(1 - ic_3)|A_R|^2 A_R - g_2(1-ic_2)|A_R|^2 A_L, \tag{1}$$

$$\tau_0(\partial_t A_L - s_0 \partial_x A_L) = \varepsilon A_L + \xi_0^2(1+ic_1)\partial_x^2 A_L - g_0(1 - ic_3)|A_L|^2 A_L - g_2(1-ic_2)|A_L|^2 A_R. \tag{2}$$

Here, A_R and A_L are the amplitude of the right and left moving waves, s_0 is the linear group velocity, and c_1, c_2, and c_3 measure the linear and nonlinear dispersion. The experimentally accessible control parameter ε measures the distance from threshold. The coefficients τ_0, ξ_0, and g_0 give the scales of time, space, and amplitude. To model our experiment, where left and right traveling waves suppress each other, and g_2 should be larger than g_0 [4].

A. Scaling

Sources show complicated behavior within the amplitude equations (1) and (2) [4,14]. For

$$\varepsilon > \varepsilon_c^{so} \gtrsim \varepsilon_{ca} = \frac{(s_0\tau_0/\xi_0)^2}{4(1+c_1^2)}, \tag{3}$$

sources are coherent structures with a well-defined shape, while for $\varepsilon < \varepsilon_c^{so}$, sources start to fluctuate and their average width scales as $\propto \varepsilon^{-1}$ (see Fig. 2). The quantity ε_{ca} in Eq. (3) is simply the value of ε, where the transition from absolute to convective instability of the $A\equiv 0$ state occurs [14,15]; its relevance can be understood as follows. Consider the dynamics of a single front in the left-moving wave amplitude A_L only, for which $A_L(x \gg 1) \rightarrow 0$. The propagation velocity of this front is given by a competition between the linear group velocity, which tends to convect any structure to the *left* with velocity s_0, and the propagation of the front into the $A=0$ state with, in the comoving frame, velocity $v^* = 2\xi_0\sqrt{\varepsilon(1+c_1^2)}/\tau_0$ [4,14]; the front velocity in the laboratory frame is thus $v^* - s_0$. Viewing a source as a pair of fronts in A_L (on the left) and A_R (on the right), it is clear that these fronts move together when $\varepsilon > \varepsilon_{ca}$, but move apart when $\varepsilon < \varepsilon_{ca}$; the change in direction of front propagation precisely corresponds in the transition from absolute to convective instability.

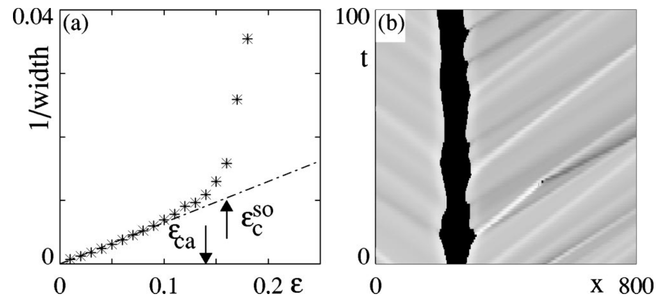

FIG. 2. Numerical results for the behavior of sources in the coupled amplitude equations (1), (2). (a) Inverse average source width as a function of ε for the coupled CGL equations (CGLE) with $s_0=1.5$, $c_1=-1.7$, $c_2=0$, $c_3=0.5$, $g_0=1$, and $g_2=2$. The coefficients s_0 and c_1 were chosen to be similar to those measured in the experiment; also $g_2>g_0$ in the experiment. The values of c_2 and c_3 were chosen such that the plane waves remain stable; their precise value does not play a significant role then. Note the crossover near $\varepsilon_{ca}=0.14$. (b) Space-time plot of the local wave number of a fluctuating source for $\varepsilon=0.11<\varepsilon_c^{so}\approx 0.14$ illustrating fluctuations of the width. In the black region, the amplitude has fallen below 10% of the saturated value; the light and dark curves correspond to holelike wave number packets sent out by the source.

Numerical simulations of Eq. (1) were done in order to see whether the experimentally observed source behavior described below could be understood on the basis of the amplitude description. Such simulations [4] have revealed that sources do *not* simply move apart and diverge when the instability of the $A\equiv 0$ state becomes convective; for $\varepsilon = \varepsilon_c^{so} \gtrsim \varepsilon_{ca}$, when the sources have become very wide, they start to fluctuate. For smaller ε, the average source width scales as ε^{-1} (see Fig. 2). The mechanism responsible for the sources staying at a finite but large average width is not completely understood and may depend on the noise strength. In the low noise limit, the "tip" regions of the two fronts sense the other mode which leads to the formation of phase slips there. The resulting perturbations are then advected by the group velocity and amplified by the linear growth rate, resulting in a jittery motion of the front. For larger noise strength, convective amplification of noise may compete with this mechanism.

These phenomena are illustrated in Fig. 2 which has been calculated for parameter values that are in the range of the experimental ones, but we emphasize that the predicted source instability is generic and insensitive to the precise parameter values.

III. MEASUREMENTS

A. Front and group velocities

Now that we have discussed the theoretical predictions for sources, we return to our experiment. For a comparison of

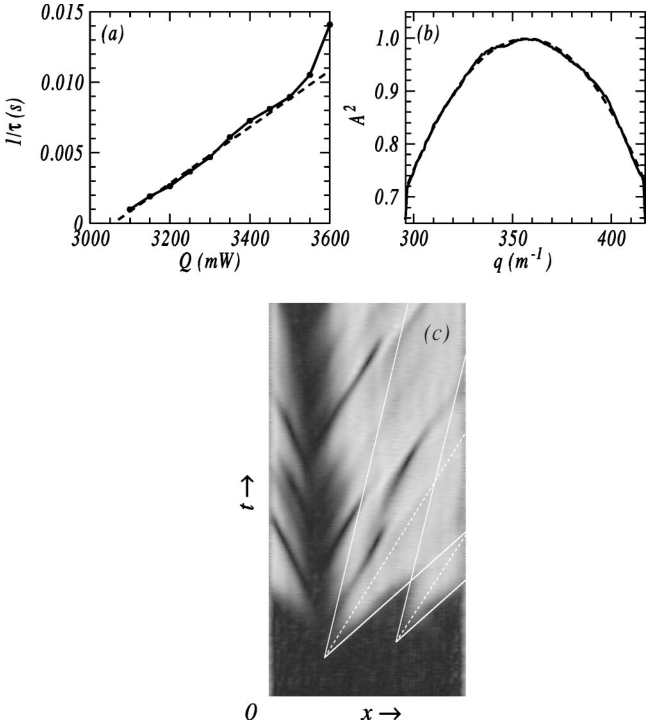

FIG. 3. Determination of the coefficients of the CGLE. (a) Time scale τ determined from the exponential growth of the amplitude in quench experiments for various values of the heating power Q. This time scales as $\tau = \tau_0/\varepsilon$, with $\tau_0 = 16(1)$ s. (b) Correlation length ξ_0. Full line: histogram of squared modulus $|A|^2$ vs q which is measured from a modulated wave field at $\varepsilon = 0.10$. Dashed line: fit of $|A|^2 = 1 - \xi_0^2/\varepsilon(q-q_0)^2$, with $\xi_0 = 2.7(6) \times 10^{-3}$ m. $|A|$ is normalized so that $|A| = 1$ corresponds to waves with wave number q_0. (c) Front velocity. Shown is the modulus $|A(x,t)|$. The x extent of the scan is 0.682 m and the total time is 5242 s. At $t = 0$, the power is quenched from $Q = 0$ to $Q = (1+\varepsilon)Q_c$, with $\varepsilon = 0.051$. The white lines outline two fronts. Since $\varepsilon < \varepsilon_c^{so}$ here, both fronts propagate in the same direction (here to the right).

the source behavior with theory, we need to determine the transition from convective to absolute instability, which requires measurements of the group velocity and the front velocity as function of ε.

The group velocity s_0 was determined from the propagation of deliberate perturbations of the surface. We found that it has the same sign as the phase velocity and that it shows only a weak q dependence, so we associate the measured value $2.1(1) \times 10^{-4}$ m s^{-1} with the linear group velocity s_0.

Fronts were made by quenching the heating power Q to a finite value $Q = (1+\varepsilon)Q_c$ at $t = 0$. After a short while, waves invade the unstable surface in the form of fronts. The boundaries of these fronts travel with $s_0 \pm v_f$, respectively, where v_f scales with ε as $v_{f0}\sqrt{\varepsilon}$. Figure 3(c) shows the evolution of the amplitude of the waves for $\varepsilon = 0.051$; this value appears to be below ε_{ca} because the velocity of the fronts has the same sign as the group velocity. The results of several experiments, both at $\varepsilon < \varepsilon_{ca}$ and $\varepsilon > \varepsilon_{ca}$ yields that $v_{f0} = 5.4(5) \times 10^{-4}$ m/s. Comparing this to the value obtained for s_0, we immediately find that $\varepsilon_{ca} \approx 0.15(5)$. An alternative estimate of ε_{ca} was made from observing at which ε the slowest moving edge of a front has zero velocity, which led to a value of $\varepsilon_{ca} = 0.10(2)$.

B. Measurements of the coefficients

In principle, a confrontation of theory and experiment can also be performed by measuring the characteristic time (τ_0) and length (ξ_0) scales, the linear group velocity s_0, and linear dispersion coefficient c_1, since from these the transition from convective to absolute instabilities also follows [see Eq. (3)]. Note that starting from the full hydrothermal equations, these coefficients can, in principle, be obtained from a systematic amplitude expansion [1]. At present we can only obtain c_1 via measurements of the front velocity which lead to a consistency check (see below). The length and time scales are relevant for comparing space-time diagrams of experiment and theory and are measured independently.

The characteristic time is determined from measurements in which the growth of the amplitude is followed when, after a sufficient long transient in which a plane wave is established, ε is increased from $\varepsilon = 0.017$ to larger values. The initial growth of $|A|$ is exponential $\sim \exp(t/\tau)$, and repeating this experiment for various values of ε yields the data presented in Fig. 3. Using the fact that τ scales as $\tau = \tau_0/\varepsilon$, we obtain that $\tau_0 = 16(1)$ s.

The length scale ξ_0 was measured from weakly modulated waves in the single-wave domains; according to Eq. (1) with $A_L = 0$, these are related by $A(q)^2 g_0 = (\varepsilon - \xi_0^2 q^2)$. Plotting these values, we obtain Fig. 3(b), in which we recognize the quadratic behavior of $|A|$ as a function of q. The measured ξ_0 differed slightly (but not systematically) from run to run and from a series of such measurements and fits we find for the correlation length $\xi_0 = (2.7 \pm 0.6) \times 10^{-3}$ m, which only close to threshold becomes similar to the basic wavelength of the traveling waves.

Taking these time and length scales and the measured front velocity v_{f0} used before, we find then that $(1+c_1^2) \approx 2.6$, from which it follows that $c_1 = \pm 1.3(4)$. A weak consistency check is that $(1+c_1^2)$ should be larger than one; independent measurements of c_1 would lead to a stronger consistency check.

IV. COMPARISON BETWEEN EXPERIMENT AND THEORY

A. Sources

Now that all relevant parameters of the amplitude equations are approximately known, we turn to the behavior of sources in our experiment. The dependence of the width $w(t)$ of sources on the control parameter ε was measured in long experimental runs, in which a source was located at large heating power $\varepsilon \approx 0.3$ and then followed at progressively smaller values of ε [18]. At each ε, the source was observed for several hours by scanning the fluid surface, while keeping the experimental conditions constant.

From the width $w(t_i)$ at discrete scan times t_i, we computed the mean $\langle w \rangle$ (as well as the standard deviation σ [18]). Figure 4 shows that the behavior of $\langle w \rangle$ as a function

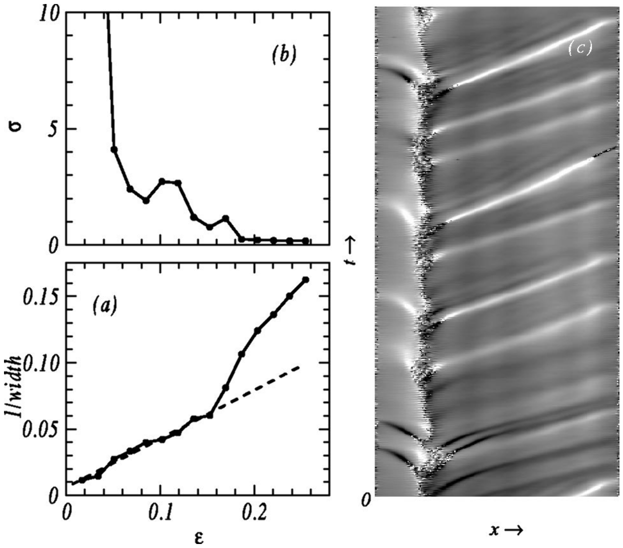

FIG. 4. (a) Dependence of the width of a source on the reduced control parameter ε. Dots, mean width $\langle w\rangle^{-1}$; and dashed line, fit of $\langle w\rangle \sim \varepsilon^{-1}$. (b) Dependence of the rms fluctuation $\sigma = \sqrt{\langle w^2\rangle - \langle w\rangle^2}$ of the width of a source on ε. Notice that the source becomes unstable for $\varepsilon > \varepsilon_{ca}$. Note that in (a) and (b), length scales have been nondimensionalized by the characteristic scale ξ_0. (c) Space-time diagram of the wave number field $q(x,t)$ of an unstable source, $\varepsilon = 0.11$; the extent of the x axis is $158\xi_0$ and the total time is $660\tau_0$.

of ε in the experiments shows the same qualitative features as the numerical simulations of Fig. 2: For decreasing ε, the width appears to diverge, but at $\varepsilon \approx 0.15$ there is a crossover to a $\langle w\rangle \sim \varepsilon^{-1}$ behavior. Below this crossover value, the sources fluctuate strongly and the standard deviation of the width rapidly increases [17]. In a cyclic fashion, these sources first grow and spawn outward-spreading wave fronts, leaving an interval of near-zero wave amplitude behind in the source core. Here phase slips occur, which make the fronts jump back; the resulting phase twists are carried away by hole structures which travel roughly with the group velocity (the light and dark lines). In our numerical simulations of the coupled CGL equations (Fig. 2), exactly the same hole structures are observed. The crossover *value* for ε_c^{so} is consistent with the transition value ε_{ca} that we determined before.

B. Holes

The structures sent out by the erratic sources display a dip in the amplitude $|A|$ and are therefore referred to as holes. It is well known that holes play an important role in the dynamics of traveling-wave systems, and that different types can be distinguished by whether the wave numbers of their two adjacent waves are similar or substantially different [2,3,7,8,11]. From the measured wave number profile in Fig. 5(a), it can be seen that the wave numbers at the back and front side of the hole are very similar. We therefore associate these holes with so-called *homoclinic holes* [3]. In addition, they display the following typical homoclinic hole behavior [see Figs. 2(b) and 4(b)]: they do not send out waves and occur quite close together, they can evolve to defects and

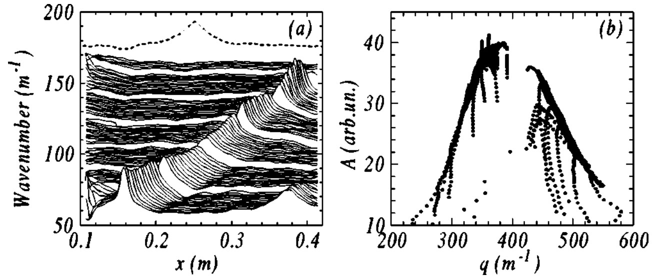

FIG. 5. (a) Wave number profile of a hole emitted from the unstable source of Fig. 4(b). Dashed line: typical wave number profile. To help with reading the wave number off the vertical axis, the plot has been sectioned. (b) Scatter plot of the minimum of the modulus vs the extreme (in x) of the wave number along each of the holes shown in Fig. 4(b). Both compression (large q) and dilation (small q) holes belong to a one-parameter family.

their propagation velocity (which in lowest order is given by s_0) depends on the value of the extremum of q. In the local wave number plot of Fig. 2, dilation holes (the dark lines) have a larger velocity than compression holes (light lines), just as in the experimental plot Fig. 4(c). In fact, the correlation between the type of wave number modulation and the velocity of these coherent structures depends on the sign of c_1, which was selected accordingly for the numerical simulations.

Since homoclinic holes are dynamically unstable, their local profiles slowly evolve along a one-parameter family; on a scatter plot of the values of the minimum of $|A|$ vs the corresponding extremum of q, these values collapse on a single curve [3]. The holes in our experiment precisely show this behavior: The extrema of $|A|$ and q rapidly evolve toward a parabolically shaped curve, and stay there during their further evolution [Fig. 5(b)]. We only observed these holes in our experiment for at most a few characteristic times—too short to see clear signs of the weak instability predicted from the CGL equation.

V. DISCUSSION AND OUTLOOK

Our experiments raise a number of suggestions, as the following, for further work.

(i) The width where sources start to fluctuate is larger in the theory $[O(100\xi_0)]$ than in experiments $[O(20\xi_0)]$, while the fluctuations appear stronger for experimental sources. Experimental noise or nonadiabatic effects which perturb the fronts may play a role here.

(ii) Earlier experiments [12] have shown that for different heights of the wire, qualitatively different behavior occurs. Systematic measurements of the coefficients as a function of height may turn the heated wire experiment into a CGLE machine with tunable coefficients.

(iii) Longer observations and more controlled generation of holes may shed more light on their relation to the homoclinic holes predicted by theory, and may show the highly characteristic divergence of lifetime as a function of initial condition [3].

(iv) Sinks show nonadiabatic phase matching and in fact posses completely antisymmetric profiles [17]; there is no clear theoretical understanding of this.

ACKNOWLEDGMENTS

We thank Ad Holten and Gerald Oerlemans for technical assistance. Financial support by EC Network Contract No. FMRX-CT98-0175, by the ''Nederlandse Organisatie voor Wetenschappelijk Onderzoek (NWO),'' and by ''Stichting Fundamenteel Onderzoek der Materie (FOM)'' is gratefully acknowledged.

[1] M.C. Cross and P.C. Hohenberg, Rev. Mod. Phys. **65**, 851 (1993).

[2] H. Chaté, Nonlinearity **7**, 185 (1994).

[3] M. van Hecke, Phys. Rev. Lett. **80**, 1896 (1998); M. van Hecke and M. Howard, *ibid.* **86**, 2018 (2001).

[4] M. van Hecke, C. Storm, and W. van Saarloos, Physica D **134**, 1 (1999).

[5] V. Croquette and H. Williams, Phys. Rev. A **39**, 2765 (1989).

[6] Y. Liu and R.E. Ecke, Phys. Rev. E **59**, 4091 (1999).

[7] J. Burguete, H. Chaté, F. Daviaud, and N. Mukolobwiez, Phys. Rev. Lett. **82**, 3252 (1999).

[8] P. Bot and I. Mutabazi, Eur. Phys. J. B **13**, 141 (2000).

[9] A. Joets and R. Ribotta, Phys. Rev. Lett. **60**, 2164 (1988); M. Rabaud, S. Michalland, and Y. Couder, *ibid.* **64**, 184 (1990); P. Habdas, M.J. Case, and J.R. de Bruyn, Phys. Rev. E **63**, 066305 (2001).

[10] N. Garnier and A. Chiffaudel, Phys. Rev. Lett. **86**, 75 (2001); N. Garnier, A. Chiffaudel, and F. Daviaud (unpublished).

[11] W. van Saarloos and P.C. Hohenberg, Physica D **56**, 303 (1992).

[12] J.M. Vince and M. Dubois, Europhys. Lett. **20**, 505 (1992); Physica D **102**, 93 (1997).

[13] The definition of sources and sinks involves the fully nonlinear group velocity [4], but in our experiments, the direction of this group velocity is equal to the direction of the *linear* group velocity s_0 [Eqs. (1) and (2)].

[14] P. Coullet, T. Frisch, and F. Plaza, Physica D **62**, 75 (1993).

[15] A. Couairon and J.M. Chomaz, Physica D **108**, 236 (1997); S.M. Tobias, M.R.E. Proctor, and E. Knobloch, *ibid.* **13**, 43 (1998).

[16] The brand name of the oil is Tegiloxan 3 produced by Goldschmidt AG (Essen, Germany). At 21 °C, it has viscosity $\nu = 3.397\times10^{-6}$ m s^{-2}, density $\rho = 892.4$ kg m^{-3}, surface tension $\alpha = 18.3\times10^{-3}$ N m^{-1}, with temperature coefficient $d\alpha/dT = -9.7\times10^{-5}$ N m$^{-1}K^{-1}$, and a refractive index $n = 1.395$.

[17] L. Pastur, M.T. Westra, and W. van de Water Physica D **174**, 71 (2003).

[18] To quantify the width of sources, we use our finding that the envelope of the experimental pattern is well fitted by the expression $S_+(x-x_0)+S_-(x-x_0)$, with $S_\pm \propto [1+a\exp(\pm 2bx)]^{-1/2}$. The source width w was defined as $S_\pm(\mp w/2) = 1/2$.